THE ASTROPHYSICAL JOURNAL, 266:160–170, 1983 March 1

ON SEARCHES FOR PULSED EMISSION WITH APPLICATION TO FOUR GLOBULAR CLUSTER X-RAY SOURCES: NGC 1851, 6441, 6624, AND 6712

D. A. LEAHY,[1] W. DARBRO, R. F. ELSNER, AND M. C. WEISSKOPF
Space Science Laboratory, NASA Marshall Space Flight Center
P. G. SUTHERLAND[2]
Physics Department, McMaster University
AND
S. KAHN AND J. E. GRINDLAY[2]
Center for Astrophysics
Received 1982 June 10; accepted 1982 August 26

ABSTRACT

We present the results of searches for periodic pulsations in the X-ray emission from four globular cluster sources, NGC 1851, NGC 6441, NGC 6624, and NGC 6712. The data were obtained by the Monitor Proportional Counter aboard *HEAO 2* (*Einstein Observatory*). The methods of analysis are presented in some detail because we have correctly accounted for several effects which have been routinely overlooked by others. The periods searched cover the range from ~ 1 ms to ~ 500 s. No pulsed emission was detected, and the (90% confidence) upper limits for the pulsed fraction are presented.

Subject headings: clusters: globular — pulsars — X-rays: sources

I. INTRODUCTION

The exact nature of the globular cluster X-ray sources remains a mystery. They are believed to be accreting neutron stars in binary systems which undergo occasional nuclear flashes on their surfaces (see, e.g., Fujimoto, Hanawa, and Miyaji 1981 for a recent review and references). Presently known neutron stars are either radio pulsars or X-ray pulsars in binary systems. In general, these possess strong magnetic fields ($\sim 10^{12}$ gauss) and are rotating so that the X-ray emission is pulsed at the rotation period. The detection of periodic pulsations from the globular cluster X-ray sources would provide conclusive evidence that the bursters are also neutron stars.

In this paper we present the results of searches for pulsed emission from the four cluster X-ray sources NGC 1851, NGC 6441, NGC 6624, and NGC 6712. These four were detected as part of a survey of globular clusters made with the *Einstein Observatory* (Grindlay 1979*a*, 1981). The cluster parameters are summarized in Table 1 and can be seen to encompass a wide range of cluster types. All of these clusters are known to be burst sources, and all of the observations were made when the sources were in their "high" or nonbursting phases.

The observations and the spectral information are discussed in § II. In § III we present the method of analysis used to search the data for periodic pulsations. This section is somewhat detailed because we have been careful to take into account several effects which arise either from the discrete binning of the data or from the fact that the pulsed signal need not be precisely at one of the frequencies searched. Both these effects are important but seem to have been ignored or overlooked by others in establishing their sensitivity to pulsed emission. The results and the upper limits to pulsations are given in § IV.

II. OBSERVATIONS

The data were recorded by the time interval processor (TIP) of the monitor proportional counter (MPC) during the spring of 1979. The instrument is described by Gaillardetz *et al.* (1978) and Grindlay *et al.* (1980). Briefly, the TIP records the time intervals between photons detected by the 667 cm^2 argon-gas–filled proportional counter in the bandwidth from 1 to 22 keV. The accuracy of the time intervals is 1 μs or 1.6%, whichever is greater, and the minimum time between events is 10 μs. The data readout is telemetry limited. The TIP utilizes a buffer memory to attempt to cope with high count rates. When the memory is full, however, no data are recorded until all the stored information is read out. This results in either 2.56 s or 0.852 s gaps in the data stream when the count rate exceeds ~ 30 or ~ 100 counts s^{-1}, respectively, depending on which of two telemetry modes is utilized. Longer gaps are, of course, also present because of the passage of the satellite through the South Atlantic Anomaly and Earth occultations.

The MPC is also equipped with eight logarithmically spaced pulse-height channels, which enable us to perform

[1] NAS/NRC Research Associate.
[2] Alfred P. Sloan Foundation Fellow.

TABLE 1

CLUSTER PARAMETERS

Cluster	Distance (kpc)	Central Density ($10^4 M_\odot$ pc^{-3})	Concentration ($\log r_t/r_c$)	Relaxation Time (10^7 yr)	Spectral Type	Metallicity (Fe/H)	Extinction (10^{21} cm^{-2})
NGC 1851	10.8	8.5	1.8	3.7	F7	−1.29	0.4
NGC 6441	10.0	13	1.7	8	G2	−0.24	3.0
NGC 6624	8.5	11	2.2	5	G5	−0.34	1.6
NGC 6712	7.3	0.15	1.2	35	G5	−0.43	2.3

NOTE.—Cluster data are from Arp 1965, Peterson and King 1975, Peterson 1976, Grindlay 1979*b*, and Harris and Racine 1979.

crude spectroscopy in the energy range 1–22 keV. Spectral analysis is accomplished by folding simple trial models through the energy response of the detector and then adjusting relevant parameters until a satisfactory fit to the data is achieved. In Table 2, we have provided an ephemeris of the observations along with our constraints on the spectrum derived in this manner. For the globular clusters, we have chosen to fit a thermal bremsstrahlung spectrum (exponential with a Gaunt factor), although satisfactory fits can also be obtained with power-law models. The relevant parameters are the spectral temperature kT and an absorption energy E_A, which is approximately related to the absorbing column density by

$$N_{\rm H} = 5.08 \times 10^{21} E_A^{2.72} .$$

Absolute 90% confidence regions for these parameters are given in the table. Also quoted is the approximate 2–6 keV intensity for each observation in *Uhuru* flux units. The uncertainty in these numbers is roughly a few percent and is dominated by systematic effects associated with the choice of a particular spectral model.

TABLE 2

SPECTRAL PARAMETERS

Cluster	Julian Day (2,443,000+)	T_1/T_2[a] (s)	R[b] (counts s^{-1})	2–6 keV Intensity (UFU)	Range in kT (keV)	Range in E_A (keV)
NGC 1851	926.882	2496/2446	32.3	9.55	8.7–11.6	0.00–0.60
	936.065	1720/1423	29.8	6.78	6.8–9.2	0.00–0.60
NGC 6441	937.680	1426/792	68.4	29.48	>19.3	0.60–1.20
	937.932	425/264	59.9	25.58	9.4–13.6	0.58–1.08
	937.937	970/497	58.1	25.48	9.0–11.7	0.70–1.19
	937.949	946/585	59.5	25.92	7.9–11.7	0.80–1.23
NGC 6624	946.913	5897/228	520.5	288.19	17.1–29.2	0.00–0.86
	947.830	5721/343	464.4	262.53	11.1–16.3	0.00–0.85
	947.902	671/47	487.9	273.59	11.8–18.3	0.00–0.79
	968.570	2800/1493	395.2	220.38	11.4–17.1	0.00–0.75
	969.236	6032/1942	373.6	219.28	12.3–17.1	0.00–0.74
	969.305	5826/1870	340.9	212.75	10.4–14.9	0.00–0.71
NGC 6712	956.079	1698/1696	25.4	4.59	3.9–4.7	0.00–0.67
	970.132	303/303	24.1	4.90	3.4–4.6	0.00–0.77
	970.139	1213/1088	25.1	4.86	3.9–4.6	0.00–0.68
	970.201	2061/2061	25.1	4.87	3.9–5.2	0.00–0.71
	970.266	2077/1694	25.5	4.82	3.9–5.2	0.00–0.67
	970.333	2047/1633	26.0	4.90	3.9–5.1	0.00–0.88
	970.398	2113/2030	27.3	4.97	3.9–4.7	0.00–0.75
	980.151	1304/1303	28.8	4.71	3.8–4.5	0.00–0.72
	980.217	2375/2332	27.6	4.87	4.5–5.4	0.00–0.53
	1145.289	324/242	25.9	6.09	3.6–5.5	0.00–1.15
	1145.295	810/726	26.9	6.79	4.8–6.3	0.00–0.73
	1145.339	1102/1060	27.4	5.98	4.8–6.1	0.00–0.64
	1145.353	1182/1181	27.4	6.77	4.8–5.5	0.00–0.62

[a] T_1 is the total elapsed time, and T_2 is the actual integration time.
[b] R is the total count rate including background, which is nominally 17.5 counts s^{-1}.

III. DATA ANALYSIS

The TIP data were converted to a series of photon arrival times. Two methods of analysis were used to examine these data for evidence of periodic pulsations. These were the fast Fourier transform (FFT) and epoch folding.

In general, both techniques have certain advantages and disadvantages in their application. These are exacerbated both by the presence of gaps in the data and the large number of statistically independent frequencies which could, in principle, be examined. Epoch folding is more sensitive to the nonsinusoidal pulse shapes encountered in X-ray astronomy. Furthermore, the technique is relatively insensitive to randomly occurring gaps in the data so long as the net pulse phase coverage is reasonably uniform. Epoch folding is, however, extremely time-consuming on the computer. (However, there are techniques to optimize the sensitivity given a limited amount of computer time, as discussed later.) The FFT, on the other hand, is extremely efficient. However, the FFT is difficult to interpret in the presence of gaps in the data unless some ad hoc technique such as "whitening" of the gaps is introduced. Although such techniques are viable in certain contexts (see, e.g., Groth 1975), we limited the use of the FFT to the examination of short continuous stretches of data.

a) The Fast Fourier Transform

The FFT has long been in existence and the algorithms are well documented and will not be repeated here (see, e.g., Jenkins and Watts 1968). In our case, a continuous segment of length T is binned into $N = 2^m$ bins, the kth bin containing m_k counts. The $\bar{m}$ is calculated and subtracted from the number of counts in each bin. The FFT is then performed on the resulting data set, yielding a power spectrum P_j at 2^{m-1}-values corresponding to the statistically independent frequencies ω_j ($\omega_j = 2\pi j/T$, $j = 1, 2, \ldots, 2^{m-1}$), where

$$P_j = 2|a_j|^2/N_\gamma\,, \quad a_j = \sum_{k=1}^{2^m} x_k \exp\,(i\omega_j t_k)\,, \qquad (1)$$

and t_k is the time label of the kth bin, x_k is $m_k - \bar{m}$, and N_γ is the total number of photons. This procedure is then repeated for all continuous segments of length T, resulting in M power spectra.

Even in the absence of periodic or secular variations in the data, the power will have a nonzero mean and exhibit variations about this mean, due to statistical fluctuations in the raw data. In Appendix A, we show that, when these fluctuations are governed by the Poisson distribution, the ensemble averaged power will be 2 (given our particular normalization, see eq. [1]), with variance

$$\text{Var}\,(P_j) = 4(1 + 1/N_\gamma)\,, \quad j = 1, 2, \ldots, N/2 - 1\,, \qquad (2)$$

which, in the limit of large N_γ, simply reduces to 4. In Appendix A we also show that in this limit, the power in a single spectrum is distributed as a χ^2 random variable with 2 degrees of freedom. We note parenthetically that the result that the mean and variance are 2 and 4, respectively, is a necessary, but not sufficient, condition that the power is χ^2_2 distributed. The power spectra calculated from the M data segments of length T are summed to yield a total power spectrum. As discussed in Appendix A, this spectrum is distributed as a χ^2 random variable with $2M$ degrees of freedom.

From the preceding, it follows that the probability that the observed power at any particular frequency (in the total power spectrum) will exceed by chance a level P_0 is given by the integrated χ^2 distribution Q,

$$Q_{2M}(\chi_0^2 = P_0) = \int_{\chi_0^2}^{\infty} p_{2M}(\chi^2) d\chi^2\,, \qquad (3)$$

where p_{2M} is the familiar χ^2 probability density for $2M$ degrees of freedom. In order to perform a period search, we must establish the power level P_0 which has a small probability of being exceeded by chance. In this we must account for all the potentially interesting frequencies that have been examined. We therefore define P_0 by choosing a (percent) confidence level c, such that P_0 has *not* been exceeded by chance given N_p periods,

$$1 - c/100 = N_p\, Q_{2M}(\chi_0^2 = P_0)\,. \qquad (4)$$

In the absence of any significant power, one is left with the problem of converting this knowledge into a meaningful upper limit. This step involves (1) adopting an assumed pulse shape; (2) accounting for the binning of the data; (3) accounting for all possible pulse phase relationships with respect to the binning; and (4) accounting for the possibility that the pulse period need not be precisely at any of the values of the statistically independent periods examined by the FFT. It is worthwhile noting that points (2) and (4), although they impact the upper limit (adversely), seem to be routinely overlooked, as evidence by the absence of any mention of them (see, e.g., Cominsky *et al.* 1980; Córdova, Garmire, and Lewin 1979).

It is customary to assume a sinusoidal pulse shape, so that the instantaneous count rate as a function of time is given by

$$r(t) = r_0[1 + A \sin\,(\omega t + \phi)]\,. \qquad (5)$$

The binned signal with mean subtracted is then

$$x_k = \frac{2r_0 A}{\omega} \sin\left(\frac{\omega T}{2N}\right) \sin\left[\frac{\omega T}{N}\left(k - \frac{1}{2}\right) + \phi\right], \qquad (6)$$

with $k = 1, 2, \ldots, N = 2^m$. We calculate the power spectrum and average over ϕ (and ignore momentarily the fluctuations due to counting statistics) to find that

$$|a_j|^2 = \left(\frac{r_0 A}{\omega}\right)^2 \sin^2\left(\frac{\omega T}{2N}\right) \times \left|\frac{\sin^2\,[(T/2)(\omega_j + \omega)]}{\sin^2\,[(T/2N)(\omega_j + \omega)]} + \frac{\sin^2\,[(T/2)(\omega_j - \omega)]}{\sin^2\,[(T/2N)(\omega_j - \omega)]}\right|. \qquad (7)$$

It is important to note that even if we restricted our-

selves to considering only $\omega = \omega_j = 2\pi j/T$, equation (7) reduces to

$$|a_j|^2 = (r_0 AT/2)^2[(N/\pi j)^2 \sin^2(\pi j/N)], \quad (8)$$

which is *frequency* dependent. The "diffraction" term in square brackets approaches unity at low frequency and falls to a value of $(4/\pi^2) = 0.405$ at the Nyquist frequency $\omega = N\pi/T$. Thus, even in this simple case, there is no single number independent of frequency that characterizes the sensitivity to pulsations. This frequency dependence is a direct consequence of the *binning* of the data. Of course, ω need not at all be precisely some ω_j. We take this into account by letting $\omega = \omega_j + \delta/T$, $-\pi \le \delta \le \pi$, and averaging over all δ. This leads to

$$\langle |a_j|^2 \rangle = \left(\frac{r_0 ATN}{2\pi j}\right)^2 \sin^2\left(\frac{\pi j}{N}\right) \times \left[0.773 + \frac{0.013}{j^2} + 0\left(\ge \frac{1}{j^4}\right)\right] \approx 0.773\left(\frac{r_0 ATN}{2\pi j}\right)^2 \sin^2\left(\frac{\pi j}{N}\right). \quad (9)$$

The expected power is obtained by (1) adding to equation (9) the additional term resulting from statistical fluctuations; and (2) converting this sum to a power through equation (1). The ensemble averaged power obtained after summing M FFTs is

$$\langle P_j \rangle = 2M\left[1 + 0.773 N_\gamma \frac{A^2}{4} \frac{\sin^2(\pi j/N)}{(\pi j/N)^2}\right] = \chi^2_{\text{noise}} + \chi^2_{\text{signal}} .$$

The sensitivity to pulsations can now be established (at a confidence level c') by determining the amplitude A such that the power exceeds the detection threshold, i.e., $\chi^2_{\text{signal}} + \chi^2_{\text{noise}} \ge \chi^2_0$, c' percent of the time. The amplitude A is determined by the solution of

$$c'/100 = Q_{2M}(\chi^2_0 - \chi^2_{\text{signal}}), \quad (11)$$

where χ^2_0 is the solution of equation (4).

b) *Epoch Folding*

The technique of epoch folding data to search for periodic pulsations is particularly useful with X-ray astronomical observations for a variety of reasons. These include the higher sensitivity to nonsinusoidal pulse shapes characteristics of X-ray pulsars. Additionally, epoch folding provides a straightforward approach to handling gaps which routinely appear in satellite data due to telemetry dropouts, passage through the South Atlantic Anomaly, Earth occulations, and, in the case of the TIP, the design of the electronics. Thus one keeps track, not only of the number of events placed in each pulse phase bin but also of the actual integration time per phase bin.

Our basic approach to epoch folding considers a data set of total length (including gaps) of T seconds, folded into n pulse phase bins at trial periods ranging from $P_{\min} = 2T/i_1$ to $P_{\max} = 2T/i_2$, with $i = i_2, i_2 + 1, \ldots, i_1$. Thus, the frequency spacing is $1/2T$, and the periods are searched in steps of the frequency resolution divided by two. The statistic S used to determine the presence of pulsations is calculated for each trial period from $P_{\min}$ to $P_{\max}$ and is

$$S = \sum_{j=1}^{n} \frac{(R_j - R)^2}{\sigma_j^2}, \quad (12)$$

where $R = N_\gamma/T'$, $\sigma_j^2 = R/T_j$, and T_j is the total integration time for the jth pulse phase bin, and T' is the sum of the T_j's. The quantity R_j is the counting rate in the jth pulse phase bin. Periodic pulsations are manifest by large values of S. In Appendix B, this choice of statistic is discussed, and we note that in the limit of large N_γ, S is a χ^2_{n-1} random variable in the absence of periodic or secular variations.

At this point, one would proceed along the lines of the discussion of the FFT, i.e., establish a threshold S_0 corresponding to "detection" at a percent confidence level c, with S_0 and c such that

$$(1 - c/100) = N_p Q_{n-1}(\chi^2_0 = S_0), \quad (13)$$

where N_p is the total number of periods searched. It is worth pointing out, however, that period searches, in general, involve establishing a boundary in a multi-dimensional space whose coordinates include the minimum period,[3] the sensitivity to pulsations, and the computer time required to perform the search. In the course of our work, we have found that it may be advantageous if, rather than searching one data set of length T, one considers M data sets of length $T_M = T/M$ and proceeds to (1) search all periods from $P_{\min}$ and $P_{\max} < T/M$ in the first set, noting all periods with $S \ge S_0$; (2) search the second set at only these periods and note any periods which continue to have $S > S_0$; and (3) continue this culling through all M data sets. The detection threshold S_0 is now set by a generalized version of equation (13),

$$1 - c/100 = N_p Q^M_{n-1}(\chi^2_0), \quad (14)$$

where N_p is now the total number of periods searched in the *first* data set, and the superscript M indicates raising Q to the Mth power.

The primary advantage of using M steps rather than one is that the number of statistically independent periods in a fixed period range is reduced, effecting a savings in computer time. The price one has paid for this savings is a reduced sensitivity. The "extra" computer time, however, can be used to extend the range of periods, effectively the minimum period, as discussed in the footnote.

Once again we consider (following custom) a sinusoidal pulse shape in order to establish the sensitivity and set upper limits. We note that the effects of binning the data, and the possibility that the pulse need not be

[3] To be precise, this coordinate is the total number of periods searched; but, because of the ever increasing number of trial periods per unit period as one goes to shorter periods, the minimum period is the principal consideration.

precisely at one of the periods searched, must again be taken into account. As before, we set $\omega = \omega_j + \delta/T$ with $|\delta| \leq \pi/2$ and calculate the mean value for S and then average over δ. We find

$$\langle S \rangle = (n-1)\left[1 + \frac{0.935}{2(n-1)} A^2 N_\gamma \frac{\sin^2(\pi/n)}{(\pi/n)^2}\right] = \chi^2_{\text{noise}} + \chi^2_{\text{signal}} \,. \quad (15)$$

where n is the number of phase bins. In arriving at equation (15), we have assumed the T_j in equation (12) are identical. This result *appears* not to have the frequency dependence exhibited by the power spectrum approach. This is a consequence of working with a fixed number (n) of phase bins, independent of frequency. In the power spectrum approach the equivalent number of phase bins is simply N/j (where j is the frequency label).

The sensitivity to pulsations is determined by the same general procedure as that used for the power spectrum. The amplitude of modulation A, which would be detected c' percent of the time at confidence c', is determined by the solution of

$$c'/100 = Q^M_{n-1}(\chi^2_0 - \chi^2_{\text{signal}}) \,, \quad (16)$$

where χ^2_0 is determined through equation (14).

c) *Simulations*

Monte Carlo simulations were performed as a check on the calculations described in the preceding sections and to ensure that any subtle effect produced by the peculiar nature of the MPC/TIP was recognized and accounted for. These simulations used Monte Carlo techniques to produce photon arrival times which were then processed by a computer version of the TIP. A second simulator, which avoided the TIP entirely and generated either a binned light curve or binned data for the FFT, was also used. Two categories of simulations were performed. The first considered only steady sources at both high and low count rates. Two typical results are shown in Figures 1 and 2, where we show the distribution of the power (the statistic S). In both cases the mean value of the power (the statistic S), its variance, and its distribution are (within statistical fluctuations) what was expected. The second category of simulations utilized an input signal consisting of a sinusoidal pulsation on a steady background in order to check the validity of equations (9) and (15). Figures 3–5 show typical results. Once again, there was excellent agreement between theory and the simulations.

d) *Search Strategy*

For any given set of observations there are innumerable ways of carrying out a period search: FFT over some range of periods, M-step epoch folding over another range, etc. In choosing a particular search strategy, the aim, of course, is high sensitivity over a wide period range within the practical limitations of the computing facilities. Unfortunately, there are a large number of free parameters to consider. The data fix the

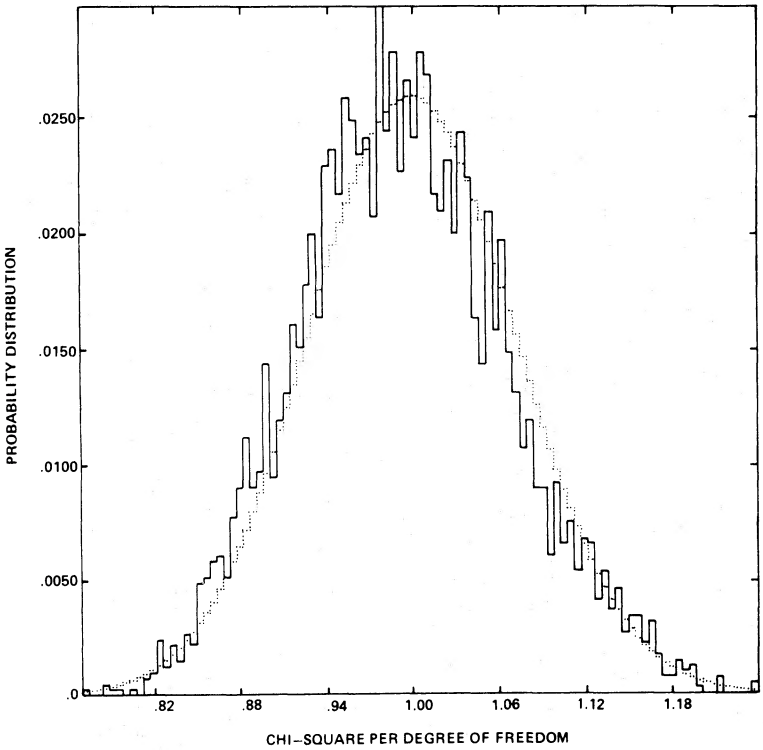

FIG. 1.—The observed (*solid line*) and expected (*dotted line*) distributions of power using the FFT. This simulation is based on a mean count rate of 404 counts s^{-1}, an experiment length of 0.5 s, 8192 bins, 4096 periods, and 192 experiments.

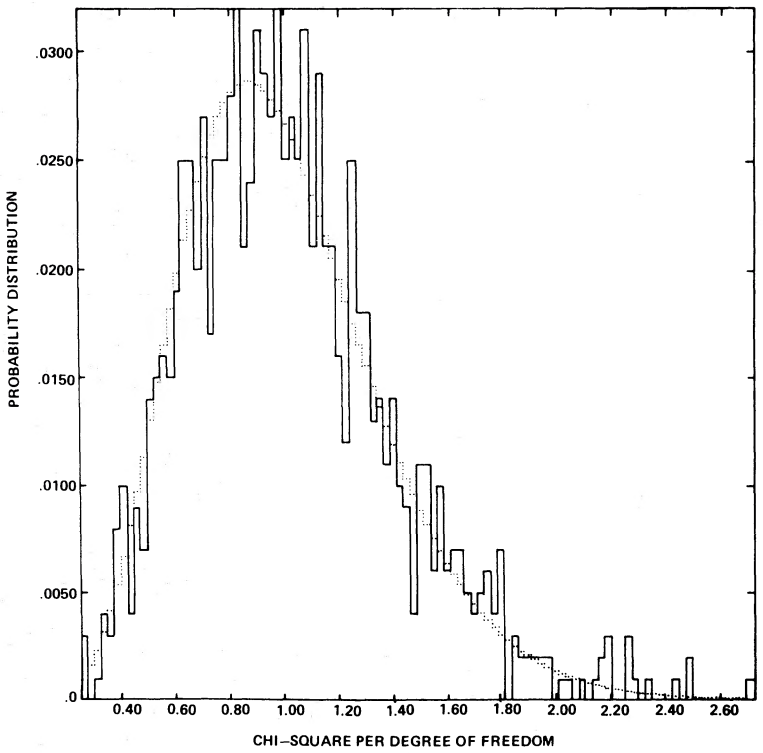

FIG. 2.—The observed (*solid line*) and expected (*dotted line*) distributions of the statistic S. This simulation is based on a mean count rate of 33.9 counts s^{-1}, an experiment length of 319 s, 1000 periods, and a 16-bin light curve.

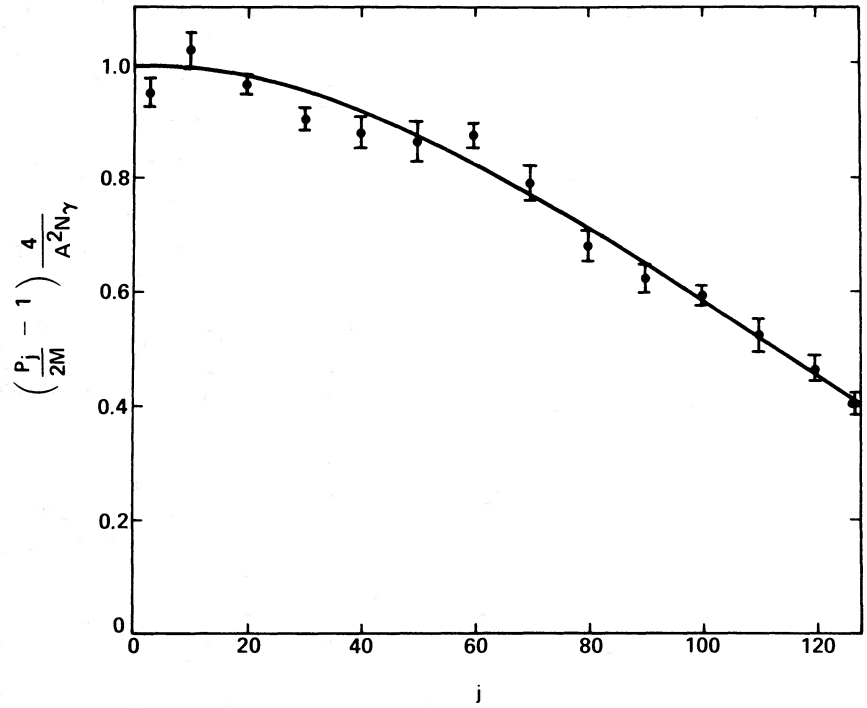

FIG. 3.—A comparison of $[(P_j/2M) - 1]4/A^2N_\gamma$ with $(\sin \pi j/N)^2/(\pi j/N)^2$ as a function of input signal frequency. The error bars are $\pm 1\ \sigma$. These simulations were based on a mean count rate of 23 counts s^{-1}, an experiment length of 128 s, 256 bins, 128 periods, 10–12 experiments, and $A = 0.5$. In all cases the input signal was precisely at one of the statistically independent frequencies.

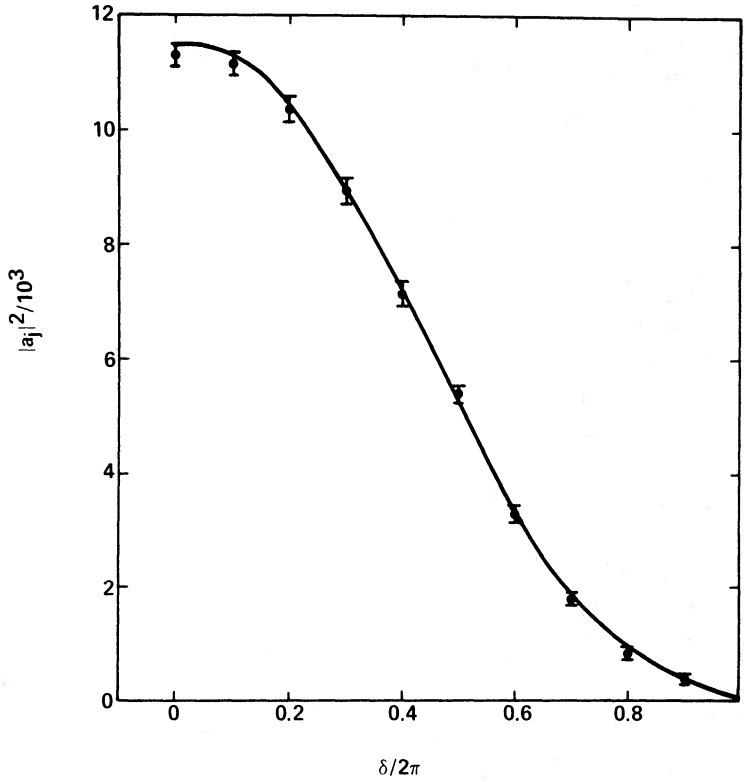

FIG. 4.—A comparison of the observed and expected power as a function of input frequency with the input frequency f_s related to the statistically independent frequency f_j through $f_j = f_s + \delta/2\pi T$. These simulations used a mean count rate of 29.9 counts s^{-1}, 256 bins, 10–11 s experiment lengths, 142–157 experiments, $A^2 = 0.5$, and $f_s = 1.0\ s^{-1}$. The error bars are $\pm 1\ \sigma$.

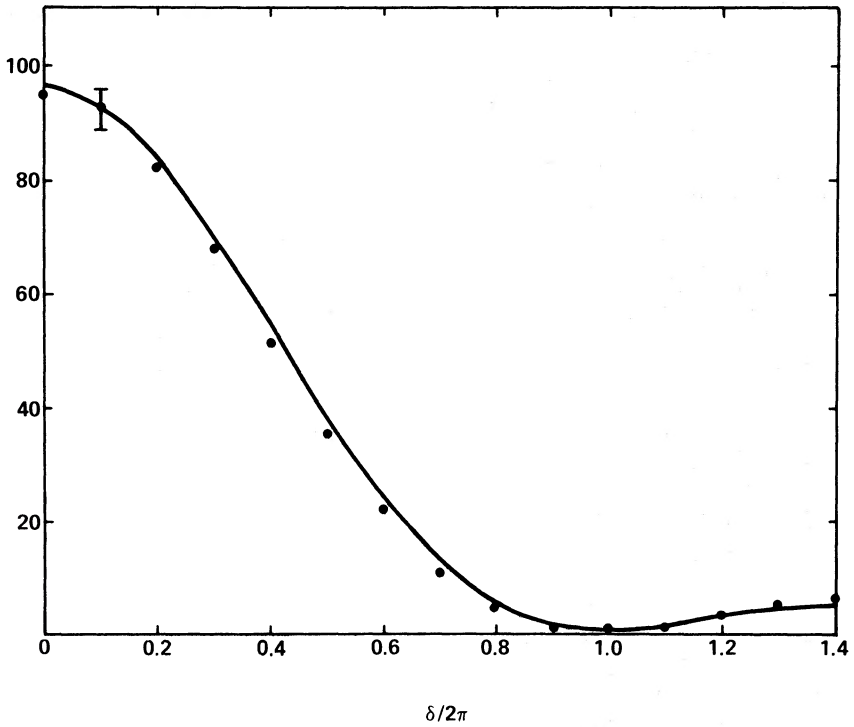

FIG. 5.—A comparison of the observed and expected values of the statistic S as a function of the input frequency with the input frequency related to the folding frequency f through $f = f_s + \delta/2\pi T$. This simulation was based on a mean count rate of 404.4 counts s^{-1}, a 16-bin light curve, an experiment length of 159 s, $A^2 = 0.25$, and $f_s = 10\ s^{-1}$. A typical $\pm 1\ \sigma$ error bar is shown.

mean count rate, and we have adopted $c = c' = 90\%$ in performing our searches. For the FFT, the principal remaining free parameters are T, M, N, and N_p, which, in turn, determine A, $P_{\min}$, $P_{\max}$, the computing time (CPU), and P_0. M-step epoch folding has as free parameters M, T_M, $P_{\min}$ (or $P_{\max}$), and N_p, which, in turn, determine $P_{\max}$ (or $P_{\min}$), CPU, and S_0. Given our fragmented data sets, we have not been able to devise an optimum search strategy. We do note that, in the unique case in which one is dealing with continuous data, it is far better to use the FFT as opposed to epoch folding; i.e., one can cover the same period range with better sensitivity with less computer time, although it should be further noted that even this conclusion is biased by choosing a sine wave as the signal for determining the sensitivity.

IV. RESULTS

Table 3 lists the results of the searches for period pulsations. The results are tabulated according to the source, the type of search performed, and the range of periods covered. There are two listings for NGC 6624, corresponding to a mean count rate of 480 counts s^{-1} (high rate) and 390 counts s^{-1} (low rate). In all cases, a nominal 17.5 counts s^{-1} background signal has been taken into account.

Two values of an amplitude of modulation are given for each source and search. The first amplitude A_1 is that which would have been considered a detection at the 90% confidence level considering only the number of periods searched for that particular search. The second amplitude A_2 is the upper limit which takes into account all the periods searched for a given source. Note that the sensitivity has only changed slightly despite the larger number of periods. A third amplitude could also have been added, that which took into account all of the periods searched. However, this result would change every time a new source was examined, and, furthermore, its value would differ little from A_2 because of the weak dependence on the number of periods.

We note here that our upper limits are based on confidence levels ($c = c' = 90\%$) such that the given pulse amplitude would lead to a threshold value of the relevant statistic, or greater, 90% of the time *and* that this threshold value has only a 10% probability of being equaled or exceeded by chance.

V. DISCUSSION

We have derived, in detail, the prescription for both searching for the presence of periodic pulsations and, if absent, the algorithms for setting upper limits. In so doing, we have taken into account all effects arising from the discrete binning of the data and the possibility that the input pulse need not be precisely at one of the frequencies searched. Both effects tend to reduce the sensitivity to pulsations independent of the method used, and, in the case of the FFT, the binning leads to frequency-dependent upper limits.

We wish to emphasize that the formal calculations presented here assume that, in the absence of pulsations, the only noise present in the data is that due to counting statistics. Other noise, produced by the X-ray source, has

TABLE 3

UPPER LIMITS TO PERIODIC PULSATIONS

SOURCE	SEARCH	T(s)	PERIOD RANGES	N_p[a]	UPPER LIMITS A_1[b]	UPPER LIMITS A_2[b]
NGC 6712.....	5-step EF	2060	2060–101	40	0.060	0.073
	FFT	236	101–0.0707	3330	0.075	0.078
	FFT	41.0	0.0707–0.0100	3512	0.101	0.104
	FFT	8.9	0.0100–0.00200	3278	0.196	0.201
NGC 6441.....	1-step EF	1430	357–75.0	31	0.044	0.055
	7-step EF	425	75.0–2.56	314	0.054	0.058
	FFT	3.50	2.56–0.000855	4095	0.116	0.116
NGC 1851.....	1-step EF	2500	2500–29.6	168	0.063	0.074
	FFT	486	29.6–0.199	2441	0.085	0.091
	FFT	44.0	0.199–0.0142	2889	0.102	0.105
	FFT	15.0	0.0142–0.00434	2400	0.131	0.135
	FFT	4.10	0.00434–0.00100	3153	0.180	0.185
NGC 6624:						
$r = 480$.....	6-step EF	341	114–0.410	1658	0.035	0.035
	FFT	0.410	0.410–0.000200	2048	0.056	0.067
$r = 390$.....	10-step EF	280	70.0–0.900	615	0.020	0.021
	FFT	900	0.900–0.000439	2048	0.052	0.052

[a] The number of periods in the FFT searches differs from a power of 2 because, where overlap in period between different searches occurs, we have taken the results from the most sensitive searches.

[b] The quantities A_1 and A_2 are discussed in the text. For the FFT searches, the quoted amplitude is $A \sin(\pi j/N)/(\pi j/N)$, where N is the total number of bins which is twice the nearest power of 2 greater than or equal to N_p.

not been taken into account. Examples of this include shot noise as is present in Cygnus X-1 or long-term aperiodic variations as have been observed in many X-ray sources. These will appear in the power spectrum or the distribution of the S statistic as deviations from the distribution expected from counting statistics. (We note here that all of the distributions obtained from our observations were consistent with those expected from counting statistics.) If such effects are present, our analysis would have to be altered. It is thus extremely important to verify the nature of the observed distribution functions before applying our formalism. There are other effects which also serve to impact the sensitivity to pulsations. These include the effects of binary motion and/or a period derivative. These reduce the sensitivity, in our case, more for epoch folding than for the FFT, because in epoch folding we used longer stretches of data. All the potential effects on period searches which may arise from the physics of the X-ray source itself cannot be included in a general analysis such as ours, but they should be kept in mind when applying our formal calculations to a particular observation.

No periodic pulsations were detected in the flux of any of the sources examined. The sensitivity, in all cases, was sufficiently high to have easily detected pulsations at those levels usually observed in any of the known X-ray pulsating binaries. Moreover, the period ranges covered include, for the most part, the range of observed pulse periods.

There are several arguments that would indicate that the globular cluster X-ray sources are, indeed, close binary systems in which matter is accreted by a neutron star. Among these are (1) the results of the analysis of the observed blackbody spectra during X-ray bursts (Swank *et al.* 1977; van Paradijs 1978; Inoue *et al.* 1981), which indicate a characteristic region the size of a neutron star; (2) the results of a statistical analysis of the positions of the X-ray sources with respect to the center of the clusters, which indicate a 2–11 $M_\odot$ system (Grindlay *et al.* 1982); (3) the recently discovered evidence for binary motion of 4U 1915−05 (White and Swank 1982; Walter *et al.* 1982), which, like the globular clusters, is an X-ray burster. If we accept the picture of accretion onto a neutron star as the source of energy for the persistent X-ray emission and thermonuclear flashes on the surface of the star as the explanation for the X-ray bursts, then why is it that no pulsations are detected in any of the systems we have examined? The simplest answer would be to attribute a weak magnetic field to the neutron star. As pointed out by Lewin and Joss in their recent review (1981, and references therein), it is precisely those neutron stars whose magnetic fields are too weak to adequately funnel the accreting matter that can undergo thermonuclear flashes. If this is the case, then it is even less surprising that no pulsations are detected when these sources are in their high states, when accretion has increased and the funneling is even weaker.

APPENDIX A

I. THE MEAN POWER

By definition

$$N_\gamma P_j/2 = \sum_{k,l} e^{2\pi i j(k-l)/N}(m_k - \bar{m})(m_l - \bar{m}) . \tag{A1}$$

It is straightforward to show that the ensemble average is

$$N_\gamma \langle P_j \rangle/2 = N\tilde{m} - (\tilde{m}/N)\sum_{k,l} e^{2\pi i j(k-l)/N} , \tag{A2}$$

where we have made use of the fact that, for a Poisson process,

$$\begin{aligned} \langle m_k m_l \rangle &= \tilde{m}^2 + \tilde{m} , \qquad k = l , \\ &= \tilde{m}^2 , \qquad k \neq l , \end{aligned} \tag{A3}$$

and where $\tilde{m}$ is the true (as opposed to the sample) mean. Since

$$\begin{aligned} \sum_{k,l} e^{2\pi i j(k-l)/N} &= 0 , \qquad j \neq N , \\ &= N^2 , \qquad j = N , \end{aligned} \tag{A4}$$

then

$$\begin{aligned} N_\gamma \langle P_j \rangle/2 &= 0 , \qquad j = N , \\ &= N\tilde{m} , \qquad j \neq N . \end{aligned} \tag{A5}$$

In performing the FFT we examine all frequencies from $j = 1$ to $N/2$, for which the $\langle P_j \rangle$ are equal. Thus,

$$\langle P \rangle = \langle \overline{P_j} \rangle = 2N\tilde{m}/N_\gamma = 2 , \tag{A6}$$

where the bar indicates an average over the relevant frequencies, and we have substituted the sample mean, (N_γ/N), as the best estimate for $\tilde{m}$.

II. VARIANCE OF THE POWER

First we must calculate P_j^2,

$$(N_\gamma^2 P_j^2/4) = \sum_{k,l,m,n} e^{2\pi i j(k+m-l-n)/N}\Big[m_k m_l m_m m_n - 2(m_k m_l m_m + m_k m_l m_n)(1/N)\sum_r m_r + (m_k m_m + 4m_k m_l + m_l m_n)(1/N^2)\sum_{r,s} m_r m_s - 2(m_k + m_l)(1/N^3)\sum_{r,s,t} m_r m_s m_t + (1/N^4)\sum_{r,s,t,u} m_r m_s m_t m_u\Big] . \quad \text{(A7)}$$

Now as $\sum_k e^{2\pi ijk/N} = 0$, $j \neq 0$, and there is such a sum in all terms except the first in equation (A7), these terms vanish. Next we note that the ensemble average

$$\langle m_k m_l m_m m_n\rangle = \delta_{klmn}\mu_4 + (\delta^n_{klm} + \delta^m_{kln} + \delta^l_{kmn} + \delta^k_{lmn})\mu_3\mu_1 + (\delta_{kl}\delta_{mn} + \delta_{km}\delta_{ln} + \delta_{kn}\delta_{lm})\mu_2^2 + (\delta^{mn}_{kl} + \delta^{ln}_{km} + \delta^{lm}_{kn} + \delta^{kn}_{lm} + \delta^{km}_{ln} + \delta^{kl}_{mn})\mu_2\mu_1^2 + \delta^{klmn}\mu_1^4 .$$

Here δ^l_{ijk} means $i = j = k \neq l$, δ^{ik}_{lm} means $l = m \neq i \neq k$, $k \neq l$, etc., and

$$\mu_1 = \langle m\rangle = \tilde{m} , \qquad \mu_2 = \langle m^2\rangle = \tilde{m}^2 + \tilde{m} ,$$
$$\mu_3 = \langle m^3\rangle = \tilde{m}^3 + 3\tilde{m}^2 + \tilde{m} , \qquad \mu_4 = \langle m^4\rangle = \tilde{m}^4 + 6\tilde{m}^3 + 7\tilde{m}^2 + \tilde{m} , \quad \text{(A9)}$$

for a Poisson process. Using equations (A8) and (A9), we find, after some computation,

$$(N_\gamma^2\langle P_j^2\rangle/4) = \tilde{m}N + 2\tilde{m}^2N^2 , \qquad j \neq N/2$$
$$= \tilde{m}N + 3\tilde{m}^2N^2 , \qquad j = N/2 . \quad \text{(A10)}$$

Thus, the variance is

$$\text{Var}\,(P_j) = \langle\overline{P_j^2}\rangle - \langle\overline{P_j}\rangle^2$$
$$= 4(1 + 1/N_\gamma) , \qquad j \neq N/2$$
$$= 4(2 + 1/N_\gamma) , \qquad j = N/2 . \quad \text{(A11)}$$

III. THE DISTRIBUTION OF THE POWER

Having derived the mean and variance of the power, it now remains to derive the underlying probability distribution. To do so, we write

$$a_j = \sum_{k=1}^{n} e^{2\pi ijk/N}(m_k - \tilde{m}) = A_j + iB_j , \quad \text{(A12)}$$

where A_j and B_j are real. It is straightforward to show that

$$\langle A_j\rangle = \langle B_j\rangle = 0 , \qquad B_{N/2} = 0 , \quad \text{(A13)}$$
$$\text{Var}\,(A_j) = N_\gamma/2 , \qquad j = 1, 2, \ldots, N/2 - 1 ,$$
$$= N_\gamma , \qquad j = N/2 ,$$
$$\text{Var}\,(B_j) = N_\gamma/2 , \qquad j = 1, 2, \ldots, N/2 - 1 ,$$
$$= 0 , \qquad j = N/2 ,$$

and therefore,

$$P_j = 2|a_j|^2/N_\gamma = A_j^2/\text{Var}\,(A_j) + B_j^2/\text{Var}\,(B_j) \quad \text{(A14)}$$

and

$$P_{N/2}/2 = |a_{N/2}^2|/N_\gamma = A_{N/2}^2/\text{Var}\,(A_{N/2}) . \quad \text{(A15)}$$

At this point we appeal to the central-limit theorem, which implies that the A_j and B_j are normally distributed since they are the sum of a set of random variables. In this case the right-hand side of equation (A14) is, by definition, a χ_2^2 random variable, and the right-hand side of equation (A15) is χ_1^2. If we now sum over M experiments, there will be $2M$ terms on the right-hand side of equation (A14) and M terms on the right-hand side of equation (A15). Thus the P_j, $j = 1, 2, \ldots, N/2 - 1$ will be χ^2_{2M} and $P_{N/2}/2$ will be χ^2_M. We emphasize that one must be careful to treat the $j = N/2$ term separately.

APPENDIX B

In the absence of pulsations, or any secular trend, the counts in each bin of a light curve obtained by folding at a given pulse period are Poisson distributed, with mean and variance best estimated by the mean number of counts per bin, $\bar{m}$. Typically in our experiments $\bar{m}$ is quite large, of the order of 2000 or more. In this case, the number of counts in the ith pulse phase bin m_i can safely be assumed to be normally distributed with their mean equal to their variance. If the m_i are normally distributed, then the statistic S,

$$S = \sum_{i=1}^{n} (m_i - m_{\text{expected}})^2 / m_{\text{expected}} , \tag{B1}$$

is χ-squared with $n - 1$ degrees of freedom. In our data, although the mean count rate should be constant in the absence of pulsations, the integration time might vary from bin to bin because of the gaps. Thus, $R_i \equiv m_i/T_i$, and $m_{\text{expected}} = RT_i$, where $R \equiv N_\gamma/T$, with T the total integration time. Substitution of these relationships into equation (B1) leads directly to equation (12) in the text.

REFERENCES

Arp, H. C. 1965, in *Stars and Stellar Systems*, Vol. **5**, *Galactic Structures*, ed. A. Blaauw and M. Schmidt (Chicago: University of Chicago Press), p. 401.

Cominsky, L., Jernigan, J., Ossmann, W., Doty, J., van Paradijs, J., and Lewin, W. 1980, *Ap. J.*, **242**, 1102.

Córdova, F. A., Garmire, G. P., and Lewin, W. H. G. 1979, *Nature*, **278**, 530.

Fujimoto, M., Hanawa, T., and Miyaji, S. 1981, *Ap. J.*, **246**, 267.

Gaillardetz, R., Bjorkholm, P., Mastronardi, R., Vanderhill, M., and Howland, D. 1978, *IEEE Trans.*, **NS-25**, 437.

Grindlay, J. 1979*a*, Center for Astrophysics preprint, no. 1249.

———. 1979*b*, in *Galactic X-Ray Sources*, ed. P. W. Sanford (Proc. NATO A. S. I. on X-Ray Astr., Cape Sounion, Greece; Cambridge: Cambridge University Press), in press.

———. 1981, in *X-Ray Astronomy with the Einstein Satellite*, ed. R. Giacconi (Boston: Reidel).

Grindlay, J., Hertz, P., Steiner, J., Murray, S., and Lightman, A. 1982, in preparation.

Grindlay, J., *et al.* 1980, *Ap. J.* (*Letters*), **240**, L121.

Groth, E. 1975, *Ap. J. Suppl.*, **29**, 285.

Harris, W., and Racine, R. 1979, *Ann. Rev. Astr. Ap.*, **17**, 241.

Inoue, H., *et al.* 1981, *Ap. J.* (*Letters*), **250**, L71.

Jenkins, G., and Watts, D. 1968, *Spectral Analysis and Its Applications* (San Francisco: Holden-Day).

Lewin, W., and Joss, P. 1981, *Space Sci. Rev.*, **28**, 3.

Peterson, C. J. 1976, *A.J.*, **81**, 617.

Peterson, C. J., and King, I. R. 1975, *A.J.*, **80**, 427.

Swank, J., Becker, R., Boldt, E., Holt, S., Pravdo, S., and Serlemitsos, P. 1977, *Ap. J.* (*Letters*), **212**, L73.

van Paradijs, J. 1978, *Nature*, **274**, 650.

Walter, F., Bowyer, S., Mason, K., Clark, J., Henry, J., Halpern, J., and Grindlay, J. 1982, *Ap. J.* (*Letters*), **253**, L67.

White, N., and Swank, J. 1982, *Ap. J.* (*Letters*), **253**, L61.

W. DARBRO, R. F. ELSNER, D. A. LEAHY, and M. C. WEISSKOPF: Space Science Laboratory, NASA/MSFC, AL 35812

J. E. GRINDLAY and S. KAHN: Center for Astrophysics, Cambridge, MA 02138

P. G. SUTHERLAND: Physics Department, McMaster University, Hamilton, ON L8S 4M1, Canada